Detection of dynamic QTLs for traits related to organoleptic quality during banana ripening

Stella Biabiany, Emilie Araou, Fabien Cormier, Guillaume Martin, Françoise Carreel, Catherine Hervouet, Frédéric Salmon, Jean-Claude Efile, Felicie Lopez-Lauri, Angélique d'Hont, et al.

Detection of dynamic QTLs for traits related to organoleptic quality during banana ripening

Stella Biabiany[1,2], Emilie Araou[1,2], Fabien Cormier[1,2], Guillaume Martin[2,3], Françoise Carreel[2,3], Catherine Hervouet[2,3], Frédéric Salmon[1,2], Jean-Claude Efile[1,2] , Felicie Lopez-Lauri[4,5], Angélique D'Hont[2,3,], Mathieu Léchaudel[5,6°], Sébastien Ricci[1,2°*]

[1]CIRAD, UMR AGAP Institut, F-97130 Capesterre-Belle-Eau, Guadeloupe, France
[2]UMR AGAP Institut, Univ Montpellier, CIRAD, INRAE, Institut Agro, F-34398 Montpellier, France
[3]CIRAD, UMR AGAP Institut, F-34398 Montpellier, France
[4]Avignon Université, UMR Qualisud, F-84916 Avignon, France
[5]Qualisud, Univ Montpellier, Avignon Université, CIRAD, Institut Agro, Université de La Réunion, Montpellier, France
[6]CIRAD, UMR Qualisud, F-97130 Capesterre-Belle-Eau, Guadeloupe, France

* For correspondence, sebastien.ricci@cirad.fr; +33 4 67 61 59 63
° These authors equally contributed to the work

Abstract

Fruit quality traits are directly linked to consumer acceptability, and thus key targets for banana breeding programs. We explored the genetic control of three major organoleptic and ripening-related traits, namely pulp acidity (pH), firmness (PF) and dry matter content (DMC), over a 7-day ripening period and three production cycles in a banana segregating population genotyped by sequencing. Significant broad-sense heritabilities were estimated with 0.77, 0.46 and 0.81 values for pH, PF and DMC, respectively. QTL detection was first performed on the whole dataset to analyze their dynamics. In a second approach, per-cycle data were considered to evaluate the stability across production cycles. Finally, a meta-analysis was performed. Various QTLs were detected, as well as many QTL colocalizations, while 12 of these QTLs were more prominent as they were detected in several approaches and/or explained over 15.0% of the phenotypic variation. Candidate genes were proposed for 10 of these QTLs. The QTL with the largest contribution to pulp acidity (R^2 = 19.3-50.6%) was located on LG1_7 on the genetic map of Pisang

Madu, i.e. a parent that is closely related to Cavendish, the world's most cultivated dessert banana cultivar group. This QTL is located on a chromosome derived from a reciprocal translocation that does not recombine in Pisang Madu, which is a favorable context for molecular marker monitoring. These first results will provide a relevant basis for marker-assisted selection in banana improvement programs.

Keywords: dry matter content, organoleptic banana quality, Musa, pulp acidity, pulp firmness, dynamic QTL

1. Introduction

Banana (*Musa* spp.) is a major economically important fruit that is grown throughout the world's tropical and subtropical regions. It is a cash crop that is sold on local and international markets, while also being staple food for several million people worldwide. Most world production is based on a few groups of cultivars derived from somaclonal variation, which is why bananas are particularly vulnerable to pests and diseases (Bakry et al. 2009). Banana cultivars are generally triploid, and sometimes diploid or tetraploid, with a basic chromosome number of x=11. They are derived from hybridization between several *Musa* species and subspecies (Carreel, et al. 2002, Perrier et al. 2009), and their genome consists of complex inter(sub)specific mosaics (Baurens et al. 2019; Martin et al. 2020a; Cenci et al. 2021). The main target of banana breeding programs is to produce disease resistant cultivars while maintaining good fruit quality.

However, banana breeding is particularly complex since cultivars need to be sterile or have very low fertility to produce seedless edible fruits, and since triploid is the most agronomically efficient ploidy level. Improving cultivars by successive crossing steps among the best cultivars is therefore not an option. Banana breeders thus use existing diploid cultivars to exploit their residual fertility and/or for artificial tetraploidization to recover fertility before crossing with wild or cultivated diploids to produce triploid cultivars. The genome complexity of banana cultivars and the lack of knowledge on the genetic determinism of the targeted traits are further banana breeding constraints. The rare QTL and GWAs studies performed so far in banana have focused on the seedless phenotype (i.e. parthenocarpy combined with female sterility, Sardos et al. 2016), bunch weight component traits (Nyine et al. 2019) and *Fusarium* wilt resistance (Ahmad et al. 2020).

Several large reciprocal translocations have been reported in Musa species and subspecies (Martin et al. 2017; Baurens et al. 2019, Dupouy et al. 2019, Martin et al. 2020b, Šimoníková et al. 2020). These translocations at an heterozygous state induce various extents of segregation distortion and recombination reduction that involve only the breakpoint region, a chromosome arm or an entire chromosome. They are frequently found at an heterozygous state in cultivars and breeding materials (Martin et al. 2020b), thereby at least partly explaining the major segregation distortions observed in the few genetic *Musa* maps developed so far (Fauré et al. 1993, Hippolyte et al. 2010; DHont et al. 2012; Mbanjo et al. 2012; Noumbissié et al. 2016).

In recent decades, ecophysiological studies have generated insight into the morphological, physicochemical and sensory characteristics of edible *Musa* varieties, in order to understand banana consumers' preferences and

facilitating breeding (Gibert et al. 2009; Bugaud et al. 2011, 2013). As for most fleshy fruit, sweetness, sourness, firmness, mealiness and aroma are the five most relevant attributes for consumer acceptance (Bugaud et al. 2011, 2016). Pulp acidity is an important aspect of banana organoleptic quality since it is related to the perception of sourness and sweetness based on the sugar-acid ratio, which has a high impact on consumer acceptability (Bugaud et al. 2016). pH is a practical measurement for high throughput phenotyping as this indicator is able to predict accurately the sensory characteristics sourness (Bugaud et al., 2013). During ripening, processes involved in the metabolism and accumulation of organic acids in pulp cells are under both genetic and environmental control (Etienne et al. 2013a, b, 2014, 2015). Pulp texture—mostly firmness and melting—is the second most important factor regarding the eating quality of bananas (Bugaud et al. 2016). Fruit texture and softening, associated with fruit cell wall disassembly during ripening, are also crucial fruit shelflife and postharvest quality factors (Brummell et al. 1999; Wakabayashi 2000). In recent decades, there has been an increased focus on the pulp dry matter content, which has been found to be linked to various quality traits, namely textural traits (Vázquez-Ovando et al., 2012; Gibert et al. 2010), soluble solids (Bugaud et al. 2009) and sugars (Phillips et al., 2021); with sugars, organic acids and non-structural carbohydrates being the main components of pulp dry mass. The dry matter content (DMC) is also a useful trait to discriminate cooking and dessert bananas (Gibert et al. 2009). The sensory texture of boiled bananas noted by consumers can be predicted by this criterion (Kouassi et al., 2021).

Phenotyping of organoleptic fruit quality characteristics is difficult and time-consuming in cultivated material and very hard to assess in fruits from wild material since they have very low pulp contents. The aim of our study was to analyze the genetic determinism of organoleptic quality traits in banana and to identify the genomic regions involved so as to be able to develop marker assisted selection for these traits and to improve breeding schemes. To this end, we performed QTL detection of three banana quality criteria: pH, firmness and DMC. This analysis was based on a segregating population obtained from a cross between two diploid parents that serve as elite genitors in several of the very few banana breeding programs existing around the world. The parent Pisang Madu is a cultivar closely related to Cavendish, the most commercially important dessert cultivar group, and the parent Galeo is a cooking banana cultivar. Phenotypic variation and heritability of the studied traits were exploited in a dynamic QTL analysis encompassing all days of the fruit ripening process and the various production cycles. The stability of QTLs across production cycles was also investigated. A meta-analysis was then performed to identify QTL

clustering and colocation, and to refine the confidence intervals. Several candidate genes related to the studied quality traits were identified and the implications of these findings for banana breeding programs are discussed.

2. Material and Methods

2.1. Plants materials

The progeny consisted of 156 individuals generated from crosses between the diploid Pisang Madu cultivar, used as female, and the diploid Galeo cultivar. This population was developed at the CIRAD Neufchateau station in Guadeloupe (French West Indies). Due to the reduced fertility observed in the parents, this population was obtained by mixing seeds produced from 5 bunches of Pisang Madu bananas (5 inflorescences corresponding to around 500 female flowers, with 100,000 ovules potentially hybridized with Galeo pollen). Embryo rescue was performed, as described by Bakry (2008), to maximize the recovery of all viable progeny. After greenhouse acclimation, the plants were transferred to the field from October 2013 to December 2014. The banana trees used for these experiments were grown in duplicated randomized blocks under the same field conditions, using plant suckers as planting material for block 2. These individuals were grown at the CIRAD Neufchateau station in Guadeloupe (elevation 250 m; andosol; rainfall 3,500 mm/year; latitude 16° 4'46.63" N, longitude 60° 35'29.35" O) using conventional field practices.

2.2. Fruit harvesting, ripening induction and sampling

Fruits were harvested from the field when the 'first yellow finger' stage was visible on the banana bunch. Postharvest fruit treatment and ripening induction were performed as described in Hubert et al. (2014). Bananas were then placed in a climatic room at 20°C for 48 h minimum. Fruits were exposed to 1,000 ppm acetylene for 24 h at 20°C to initiate ripening. After treatment, fruits were kept at 20°C and ambient humidity during the phenotyping phase. For each production cycle, at least 60 fruits were sampled per bunch.

2.3. Physicochemical measurements

The progeny was studied during three successive production cycles for the three distinct criteria. Measurements were performed over a 7-day ripening period (day 0 = the day of ripening initiation), each day for

pulp pH and firmness, and at days 1, 3 and 7 for pulp dry matter content (DMC). For each biological replicate (corresponding to one harvested bunch), three analytical replicates (corresponding to three fruits) were performed for pulp firmness, while two analytical replicates were performed for pulp pH and DMC. Rheological characteristics for pulp firmness was assessed using a TA-XT2 penetrometer with a 20 mm cylindrical probe on fresh banana, as described by Chillet et al. (2008). The pulp pH and DMC were measured on two of the three fruits used in the rheological analysis. The pulp pH was measured by direct insertion of a pH sensor into transversely cut fruit pulp. DMC was determined by measuring the weight loss of 2 g of fresh pulp after oven drying at 70°C for 16 h.

2.4. Phenotypic data analysis, BLUPs and heritability

All statistical analyses were performed using R software v.2.9.2 (R development Core team, 2020, http://www.R-project.org), except for the mixed linear model, which was built using PROC MIXED in SAS software, Version 9.4 (SAS Institute Inc., Carey, NC, USA). The phenotypic data were checked visually for their normal distribution and descriptive statistics were generated, including mean, range and standard deviation (SD). Pearson correlation coefficients for the measured traits within and between cycles were also calculated using the cor.test() function. The effect of genotype, days, cycle and their interactions on the organoleptic variables was estimated using the following global mixed model, which was selected according to minimization of Akaike's information criterion (AIC) (Akaike, 1974):

$$P_{ijkf} = \mu + G_i + D_j + B_k + C_f + (G\times D)_{ij} + (G\times C)_{if} + \varepsilon_{ijkf} \quad (1)$$

where P_{ijk} is the phenotypic value of genotype i at the ripening day j, for the production cycle k and the block f. μ is the overall mean of the progeny, G_i is the random effect of genotype i, D_j is the fixed effect of the ripening day j, B_k is the random effect of the block k, C_f is the random effect of the production cycle k, $(G\times D)_{ij}$ and $(G\times C)_{if}$ are their random interactions and ε_{ijkf} is the random residual error effect.

The residual distribution normality was checked afterwards. Broad-sense heritability (H^2) was then calculated using the equation proposed by Cullis et al. (2006) for unbalanced data:

$$\underline{H_C^2} = 1 - \frac{\bar{\upsilon}BLUP}{2\sigma_g^2} \quad (2)$$

where σ_g^2 is the genotypic variance, $\bar{\upsilon}BLUP$ is the mean variance of a difference of two best linear unbiased predictions (BLUPs; Henderson, 1950).

145

146 *2.5. Ploidy assessment*

147 The nuclear DNA content of the progenies (i.e, 156 offspring) and the two parents was assessed by flow
148 cytometry. A leaf sample of each plant was chopped with leaf tissue of *Oryza sativa* L. ssp. *japonica* cv. Nipponbare
149 as internal reference in modified LB01 buffer (Doležel et al. 1989) in which mercaptoethanol was substituted by 40
150 mM sodium sulfite (Na_2SO_3). Analyses were performed with a PAS II flow cytometer (Partec GmbH, Münster,
151 Germany), as described by Doležel and Bartoš (2005).

152

153 *2.6. Parentage verification*

154 Young leaves of the 156 F1 individuals and parents were sampled, and DNAs were extracted from 3 g of
155 leaf material ground in liquid nitrogen according to the modified CTAB/MATAB method (Risterucci et al. 2000).
156 Parentage verification was performed using a total of 15 SSR loci spread over the 11 *M. acuminata* chromosomes
157 based on the DH-Pahang reference genome sequence (Lagoda et al. 1998; Hippolyte et al. 2010; D'Hont et al. 2012).
158 Genotyping was carried out using the protocol described by Christelová et al. (2011) and the Applied
159 Biosystems_3500xL Genetic Analyzer and GeneMapper v4.1 software (Applied Biosystems;
160 www.appliedbiosystems.com). Automated data scores were corrected by manual checks.

161

162 *2.7. High-throughput genotyping and genetic mapping*

163 Genotyping by sequencing (GBS) libraries were constructed using the PstI and MseI restriction enzymes
164 and sequencing was performed at the GeT-PlaGe platform (https://get.genotoul.fr/) using the Illumina Hiseq3000
165 sequencer. Raw GBS sequencing data from the F1 progeny were demultiplexed using GBSX version 1.2 (Herten et
166 al. 2015) and adaptors were removed with cutadapt (Martin 2011). Variant calling was performed using the
167 vcfhunter toolbox (available at https://github.com/SouthGreenPlatform/VcfHunter/) (Garsmeur et al., 2018) as
168 described in Dupouy et al. (2019). Mapping was performed on the *M. acuminata* reference sequence assembly,
169 version 2 (Martin et al. 2016). For each accession, sites with read depths of <10 and >3,000 were excluded. The
170 procedure performed to select SNPs useful for the construction of both parental maps is schematically presented in

171 Supplemental Fig. 1. SNP markers with >10.0% missing data and individuals with >30.0% missing data were
172 removed from the mapping dataset to avoid loss of accuracy during the genetic mapping process.

173 The remaining SNPs were separated into 3 sets of markers to create parental maps for cv Pisang Madu and
174 cv Galeo using JoinMap 5.0 (Van Ooijen, 2006): lm × ll (markers from the female parent), nn × np (markers from the
175 male parent), and hk × hk markers (markers heterozygous in both parents). Parental markers were phased and
176 extracted for use as a cross pollinated population type. SNPs included in these three classes were then merged in one
177 file and used to construct the two parental maps. All identical loci were removed and then linkage groups were
178 determined with a LOD threshold of 15, a recombination fraction threshold of 0.35, a ripple value of 1.0 and a jump
179 threshold of 1.0. Markers were ordered using the regression-based parameters; and Kosambi's mapping function was
180 used to calculate genetic distances among loci (Kosambi, 2016).
181
182 *2.8. QTL detection and meta-analysis*

183 In the present study, two QTL mapping approaches were applied on the best linear unbiased predictors
184 (BLUPs) extracted from the selected mixed linear model (Equation 1). When significant, BLUPs for the GxD and
185 GxC interactions, according to the studied step, were computed for each day and cycle. Quantitative trait loci
186 analysis was performed using the multi-QTL model (MQM) in R/qtl (Broman and Sen 2009; Arends et al. 2010) and
187 interval mapping based on the marker distance. The stepwise QTL function was used to conduct a forward-backward
188 search and account for epistasis with a maximum of 5 QTLs. For each trait, the LOD threshold at a significance level
189 of $p = 0.05$ was calculated based on 1,000 permutations. QTLs with a LOD above the threshold of 3 were declared
190 significant. The percentage of phenotypic variance explained (R^2) of a single QTL was estimated based on a
191 maximum likelihood estimation, and those with a $R^2 \geq 15.0\%$ were considered as major QTLs.

192 All QTL analyses were performed for each day of the ripening process. The two QTL mapping approaches
193 were applied independently for each trait, while the meta-analysis was performed with the three traits pooled. In the
194 first approach, QTL detection was performed on the whole dataset, including all of the production cycles, to study
195 QTL stability during fruit ripening. In the second approach, QTL analysis was performed on the three cycle datasets
196 (C1, C2 and C3) separately to assess the stability of QTLs across these production cycles. For a given trait, when a
197 QTL was detected in the same region at different days of the ripening process, they were pooled into a single QTL
198 (consensus QTL), and the consensus QTL was then refined using BioMercator software V4

199 (http://moulon.inra.fr/index.php/en) and then named 'consensus QTL', with the following nomenclature:
200 Trait'datasetID'QTL-'MapName''LinkageGroup ID'. For example, DMC^{W}QTL-PM5 corresponds to a QTL related to
201 DMC detected from Pisang Madu polymorphism on linkage group 5 in the whole dataset. The meta-analysis
202 performed using BioMercator software V4 was based on QTLs obtained from the two first approaches. Five different
203 meta-analysis models (1-, 2-, 3-, 4-, or N-QTL) are proposed on BioMercator® and the best model choice was based
204 on Akaike's information criterion (AIC) values (the model with the lowest AIC-value was considered optimal).
205 Finally, the consensus QTL presented by the optimum model was considered and named MQTL (Arcade et al.
206 2004).
207
208 *2.9. Identification of potential candidate genes*

209 Research on potential candidate genes was only performed on QTLs and MQTLs showing a confidence
210 interval of 10 Mb or less. Genes coding for enzymes or transporters directly linked to acids, sugars, cell wall and
211 hormone metabolism were assessed according to Gene Ontology terms related to these functions available at
212 http://geneontology.org/. From the functional annotation of the Banana Genome Hub (BGH, https://banana-genome-
213 hub.southgreen.fr/) a systematic search of the location on the physical map of the list of identified GO terms was
214 conducted. Colocation between a QTL and a candidate gene was identified when the latter was located in the
215 confidence interval of the consensus QTL or MQTL using the BEDTools intersect function (Quinlan and Hall 2010).
216
217 2.10. *Identification of chromosomal structures associated with pH variation*

218 Both Pisang Madu haplotypes for chromosome 1 were searched in the progenies using the methodology
219 described in Martin et al. (2020b). Two classes of individuals were obtained for each of these structures: individuals
220 with haplotype 1 of Pisang Madu (with the 1/7 translocation) and individuals with haplotype 2 of Pisang Madu (with
221 the reference sequence structure). For each of these classes, the mean pH at day 7 (corresponding to ripe fruit) and
222 standard deviation were calculated. These values were then plotted using a box plot representation. pH averages for
223 the two haplotypes were compared using the Tukey test.
224
225 **3. Results**

3.1. Genotyping and genetic map

The progeny consisting of 156 individuals was genotyped by sequencing, resulting in 2.4 million polymorphic SNPs after variant calling (Supplemental Fig. 1). Seven individuals were removed from the dataset due to the extent of missing data (> 20.0%). After the filtering steps, 4,663 bi-allelic SNPs were kept, with 1,250 (6.4%) corresponding to SNPs heterozygous only in Galeo, 2,287 (11.6%) to SNPs heterozygous only in 'Pisang Madu', and 1,126 (5.7%) to SNPs heterozygous in both parents. Loci were further separated into two sets of uniparental configurations to create parental maps. Linkage groups (LGs) were named according to the reference *M. acuminata* genome assembly (D'Hont et al. 2012).

The Galeo genetic map (Supplemental Table 1), consisted of 1,148 SNPs assembled in 11 linkage groups, as expected. They were distributed among 937 independent loci due to cosegregation. The map had a total length of 1,345 cM, corresponding to an average interval of 1.5 cM between markers. However, several gaps larger than 10.0 cM or 20.0 cM were observed (Supplemental Table 1). Comparison of the genetic positions of the markers to the physical ones on the *M. acuminata* reference genome assembly v2.0 (data not shown), revealed no large genome rearrangements in Galeo compared to the reference genome assembly. This also showed that the genetic map covered 379 Mb overall, corresponding to 95.4% of the *M. acuminata* genome assembly v2.0.

The Pisang Madu genetic map (Supplemental Fig. 1) consisted of 1,319 SNPs distributed among 990 independent loci assembled in 10 linkage groups. The Pisang Madu map had a total length of 1,154 cM, corresponding to an average interval of 1.5 cM between markers. However, several gaps larger than 10.0 cM or 20.0 cM were observed (Supplemental Table 1). Comparison of the genetic positions of the markers to the physical ones on the *M. acuminata* reference genome assembly v2.0 revealed that all markers corresponding to reference chromosome 1 were genetically mapped in the middle of a linkage group that corresponded to reference chromosome 7. This linkage group was named LG1_7 (Supplemental Table 1, Fig. 1a). In addition, no recombination was detected between markers from reference chromosome 1. The genetic map covered 359 Mb, corresponding to 97.4% of *M. acuminata* genome assembly v2.0 (Supplemental Table 1).

3.2. Analysis of phenotyping data

The 156 individuals of the studied progeny were phenotyped during fruit ripening for three quality traits measured in the pulp, i.e. pH, firmness and DMC, during three cropping cycles (Supplemental Table 2). 147, 125, and 46 progeny individuals were phenotyped at cycles 1, 2 and 3, respectively. Phenotypic data of progeny individuals showed a wide distribution for all traits during fruit ripening (Fig. 2). Marked variations in pH and DMC were measured at each fruit ripening day, while for PF there was very little variation within the progenies after day 3. For each trait at each ripening day, the phenotypic data tended towards a normal distribution, except for PF which showed a right-skewed distribution from the third ripening day (Fig. 2e-h). The range of values measured for these traits and the slopes observed during fruit ripening were similar between cycles, as confirmed by the non-significant cycle effect (Table 1 and Fig. 3).

Variance analysis and decomposition (Table 1) revealed highly significant genotypic effects ($p < 0.0001$), as well as high interaction effects between genotype and the ripening day and genotype and the plant cycle ($p < 0.0001$). The proportions of variance explained (PVE) by the different factors were, however, extremely variable between traits. Genotypic effects were the strongest ones for DMC and pH (61.3% and 39.0%, respectively), but explained the lowest part of variance for PF (12.2%). Similarly, the interaction between the genotype and ripening day ranged from 7.5% for DMC to 23.4% for PF. The PVE of the interaction between the genotype and crop cycle was more stable, varying from 13.7% for DMC to 18.5% for PF. DMC and pH finally displayed high heritability values, of 0.81 and 0.77, respectively, whereas PF had the lowest one, with a value of 0.46 (Table 1).

The curve of pulp acidity determined from the pH measurements first decreased until the fourth ripening day, and then stabilized over a period corresponding to the beginning of the second part of fruit ripening process, followed by a rise until the end of ripening, i.e. generally considered as the ready-to-eat stage (Fig. 2a-d, Supplemental Fig. 2a). The pH increase was especially marked in Pisang Madu pulp, contrary to Galeo in which it remained low. PF showed a quick decrease until day 4 of ripening and then stayed almost unchanged at low values during the second part of fruit ripening until the end of this process (Fig. 2e-h, Supplemental Fig. 2b). The DMC tended to decrease during fruit ripening, with quite low variations compared to the other traits (Fig. 2i-l, Supplemental Fig. 2c). All quality traits were found to be positively correlated, regardless of the fruit ripening day, except for DMC and pH at day 7 (Table 2). Furthermore, pH had the highest correlation with PF at days 1 and 3 ($r = 0.48$), while the correlation between PF and DMC was intermediate and relatively similar for the three measurement days ($r = 0.3$ to 0.39).

3.3. QTLs detected for each of the three quality traits over the ripening period

The QTL detection results obtained with the whole dataset (first approach) are summarized in Supplemental Table 3 and Fig. 3a. A total of 36, 15 and 10 significant associations were detected for pH, PF and DMC, respectively, which corresponded to 5, 4 and 2 consensus QTLs (QTLs detected in the same region at different ripening days), respectively (Supplemental Table 3). They were located on all linkage groups (LG), except LG2. More QTLs were detected in Pisang Madu than in Galeo, except for PF. Variations in R^2 values were observed for several QTLs detected during fruit ripening (Supplemental Table 3). Most of the QTLs were not detected every day of the ripening period, many (43.0% for Pisang Madu polymorphism and 30.0% for Galeo polymorphism) were detected only for one or two days. The number of QTLs detected each day ranged from 1 to 10, with the highest number detected at the end of the ripening period (Pisang Madu map). The R^2 values determined for a single QTL, depending on the ripening day, ranged from 2.2 to 50.6% for pH, 7.9 to 30.0% for PF, and 6.8 to 26.1% for DMC (Supplemental Table 3).

For pulp pH, QTLs were detected on LG1_7, 3, 4, 6, 9 and 10 (Fig. 1b and Fig. 4). On LG1_7 of Pisang Madu, QTLs were detected in two distinct regions (Fig. 1b-c). QTLs detected in the central region of LG1_7 were detected for all fruit ripening days (pH^WQTL-PM1-7.1: R^2 = 19.3-50.6 %, CI = 27.4 Mb). This central region of LG1_7 corresponded to the part of the reference chromosome 7 and the entire reference chromosome 1 that does not recombine in Pisang Madu (Fig. 2a-c). The second region at the bottom of the LG1_7, corresponding to reference chromosome 7, was detected for all fruit ripening days, except for days 0 and 6 (pH^WQTL-PM1T7.2: R^2 = 3.2-6.9 %, CI = 2.2 Mb). These QTLs combined with those detected for pH reached a total R^2 value of 67.8% for day 6 and 58.5% for day 7.

For pulp firmness, QTLs were detected on LG1, 3, 4, 5, 6, and 11 (Fig. 1b and Fig. 4). The total R^2 values of QTLs for PF ranged from 17.7% at day 3 (2 QTLs) to 53.8% at day 6 (4 QTLs). Similar values of QTLs for PF were found at days 5 (R^2 = 47.2%; 2 QTLs) and 7 (R^2 = 41.5%; 3 QTLs). QTLs with high R^2 values (Table 3 and Supplemental Table 3) were observed for PF close to the end of fruit ripening, i.e. on LG6 at day 5 (PF^WQTL-G6: R^2 = 30.0%, CI = 9.4 Mb) and on LG11 at days 6 and 7 (PF^WQTL-PM11: R^2 = 14.2-17.8%, CI = 1.0 Mb).

For pulp dry matter content (DMC), QTLs were detected on LG5, 6, 8, 9, 10, and 11 (Fig. 1b and Fig. 4). Total R^2 values were 60.4%, 31.4% and 59.2% at days 1, 3 and 7, respectively, corresponding to 5, 2 and 5 distinct

QTLs, respectively (Supplemental Table 3). Two QTLs with major effects (Table 3) were detected at the top of LG9 on the Pisang Madu map, i.e. the first one at days 1 and 3 (DMC^{W}QTL-PM9.1: R^2 = 18.0-22.1%, CI = 0.9 Mb), and the second at day 7 (DMC^{W}QTL-PM9.2: R^2 = 26.1%, CI = 1.2 Mb).

Several QTLs for the different quality traits were found in the same regions. Two colocalizations were identified on the Pisang Madu map, i.e. at the top of LG3 with QTLs for pH and PF, and at the top of LG9 with QTLs for pH and DMC. One colocalization was identified from Galeo polymorphism at the bottom of LG6 with QTLs for pH and PF (Supplemental Table 3).

3.4. Consistency of QTLs throughout production cycles over the ripening period

QTL stability over the successive production cycles was investigated by comparing consensus QTLs detected in the same region at different ripening days throughout all cycles to those detected at each cycle (second approach). 110 cycle-specific QTLs were detected overall, including 21, 35 and 54 for cycles 1, 2 and 3, respectively (Fig. 2b-c and Supplemental Table 4). The maximum number of QTLs (51) was detected for PF, followed by pH (39 QTLs) and DMC (20 QTLs) (Fig. 2b-c and Supplemental Table 4). The detected QTLs were usually specific to one cycle (Supplemental Table 4). Six QTLs detected at one cycle were also detected at a second cycle, i.e. one for pulp pH and the others for the PF trait. Two consensus QTLs (PF^{W}QTL-G1 and pH^{W}QTL-PM1_7.1) were identified for all cycles (Fig. 1b, Fig. 4, and Table 3). Ten of the 23 QTLs found in the whole dataset (Supplemental Table 3) were detected using the cycle-specific approach (Table 3). In addition, QTL detection at each cycle allowed the identification of eight additional consensus QTLs that were not detected in the first approach, i.e. two for pH, five for PF and one for DMC. Unlike the first approach, QTLs on LG2 were detected for each trait via this cycle-specific analysis (Supplemental Table 4).

3.5. QTL meta-analysis

Interestingly, many QTLs detected in this study colocalized within or between traits, and several were overlapped, thereby increasing the size of the confidence interval. Thus, to mine MQTLs and refine QTL intervals, all QTLs from the two approaches were pooled and projected on each map to run a meta-analysis. MQTLs were projected on a consensus map in Biomercator.V4 except for LG1_7. The meta-analysis results are shown in

335 Supplemental Table 5. The meta-analysis successfully reduced the number of QTLs to investigate in this study as
336 well as their confidence intervals. A total of 33 MQTLs were distributed unevenly across the genome, 9 of which
337 were related to QTLs detected using both the first approach on the whole dataset and the cycle-specific approach
338 (Fig. 4 and Table 3). Among the MQTLs (Supplemental Table 5), three were related to pH only (MQTL-G5.2,
339 MQTL_PM1_7.3, MQTL_PM3.2), and five were related to PF only (MQTL-G4.1, MQTL-G8.1, MQTL-G9.2,
340 MQTL-PM10.1 and MQTL-PM11.2). Remarkably, the confidence intervals obtained for MQTL-PM8.1 and MQTL-
341 PM11.2—both related to DMC—were at least 85.0% lower than that detected for the whole dataset (DMC^{W}QTL-
342 PM8_1: R^2 = 9.9%, CI = 28.8 Mb; and DMC^{W}QTL-PM11: R^2 = 13.5%, CI = 19.2 Mb).
343 The number of MQTLs per LG ranged from one MQTL on LG2 to six on LG10. MQTL-G1 as well as
344 MQTL-PM8.2 covered eight QTLs, while MQTL-PM9.1 and MQTL-PM7.2 covered 15 and 18 QTLs, respectively.
345 Many of the MQTLs identified in this study were associated with two or three traits. 13 of these MQTLs were related
346 to pH and PF, 3 to pH and DMC, and 3 to PF and DMC. Moreover, 4 MQTLs were found to be related to all traits
347 (Supplemental Table 5).
348
349 *3.6. Colocalization between QTLs and candidate genes (with CI lower than 10 Mb)*
350 Colocalization between QTLs linked to pH and a selection of candidate genes culled from the literature
351 allowed the identification of genes potentially involved in pulp organic acid metabolism (Table 3, Supplemental
352 Tables 3 and 5). On the Pisang Madu map, genes related to PEPC and PEPCK were identified in the pH^{W}QTL-PM9
353 and pH^{W}QTL-PM1_7.2 confidence intervals. In addition, the latter detected by MQTL analysis, i.e.
354 MQTL_PM1_7.3, was associated with genes involved in Aco, GAD and Mal activities (Table 3 and Supplemental
355 Table 5). The gene related to V-ATPase was identified in a QTL detected by the two approaches and in the MQTL-
356 PM3.2 confidence interval (Table 3). On the Galeo map, most of these genes were identified in pH^{W}QTL-G10 and
357 MQTL-G5.2 confidence intervals (Supplemental Tables 3 and 5). Surprisingly, no candidate gene linked to citrate
358 synthase was found for all QTLs linked to pH.
359 Candidate genes involved in cell wall metabolism (division and expansion) and hormones regulating fruit
360 ripening were detected in seven QTLs linked to PF. Most of these genes were related to auxin regulation and
361 peroxidase activity, as for PF^{W}QTL-PM11 and PF^{W}QTL-G6 and for MQTL-G4.1 (1 Mb) (Tables 3 and
362 Supplemental Table 3). In addition, candidate genes involved in the ethylene response (ETR) were identified for

363 PF^{W}QTL-G11 (1.5 Mb) (Table 3). Genes involved in cell wall metabolism were found in QTL intervals on both
364 parental maps, PF^{W}QTL-PM3 and PF^{W}QTL-G6, and on several MQTLs related to several quality traits, including
365 PF.

366 Based on their functions, enzymes involved in glycolysis, sugar metabolism, transport, and specific
367 hormonal activity constituted obvious candidate genes for DMC. Candidate genes involved in cell walls—
368 corresponding to structural dry matter—were detected on two QTLs from the Pisang Madu map, i.e. PF^{W}QTL-
369 PM9.1 and -PM9.2 (Table 3). Five MQTLs linked to DMC colocated with genes coding for enzymes catalysing
370 carbohydrate synthesis or degradation (Supplemental Table 5). The same MQTLs except for MQTL-M11.2
371 colocated with aconitate hydratase activity (Aco). Sucrose synthase activity (SuSy) colocated with MQTL-PM4.1
372 and MQTL-PM9.3, while UDP colocated with MQTL-PM4.1 and MQTL-PM11.2. In addition, genes linked to auxin
373 metabolism colocated with the two MQTLs linked to DMC only (MQTL-G7 and MQTL-PM11.2).
374
375 3.7. *Identification of chromosomal structures associated with pH variation*

376 The QTL detected for pH with the greatest effect (pH^{W}QTL-PM1_7.1) was identified on LG1_7 of Pisang
377 Madu (Fig. 2b-c). Pisang Madu is structurally heterozygous for translocation between reference chromosomes 1 and
378 7. We analyzed the correlation between the presence of each of these chromosome haplotypes (chromosome 1 vs
379 chromosome 1T7) with the pH at day 7—corresponding to the ready-to-eat stage—in the population. In the progeny,
380 the mean pH calculated on individuals with chromosome 1T7 was significantly higher than that for individuals with
381 chromosome 1 (Fig. 2d). The higher pH of pH^{W}QTL-PM1_7.1 was thus associated with chromosome 1T7.
382
383 **4. Discussion**
384 *4.1. Dynamic QTL mapping approaches and meta-analysis for banana quality traits*

385 The phenotypic data analysis revealed high heritability values for two of the measured traits (≈ 0.8 for pulp
386 pH and DMC~), and a slightly less one for pulp firmness (0.46), which were suitable for further QTL detection. We
387 detected significant genotypic effects, but also strong genotype–production cycle and genotype–ripening day
388 interactions. This led us to implement two QTL mapping approaches. The first one exploited the whole dataset to
389 analyse QTLs over the fruit ripening period, as reported in dynamic QTLs analyses for other fruits (peach (Desnoues

et al., 2016), apple (Costa et al., 2010) and tomato (Sun et al., 2012)). The second one exploited data by cycle to evaluate the stability of the detected consensus QTLs according to the production cycle. These approaches resulted in detection of numerous QTLs, but the confidence intervals were broad, and lot of them were overlapping. So an additional meta-analysis of QTLs identified in these approaches was performed that enabled us to refine the QTL intervals and study potential QTLs colocalization. Meta-analysis approaches were initially developed to identify fine consensus QTLs across multiple studies for a single trait (Wu and Hu 2012), but they were also recently used to study colocalization between QTLs for distinct traits (Shen, Xiang et al. 2018)

The construction of the two parental genetic maps, used to perform QTL detection, led to 11 linkage groups for Galeo as expected, but to only 10 linkage groups for Pisang Madu, with LG1_7 associating markers from reference chromosome 1 as well as reference chromosome 7 (Fig. 2). This particularity was linked to the presence of a large reciprocal translocation involving reference chromosomes 1 and 7 that has been reported in heterozygous state in Pisang Madu and that prevents recombination on chromosome 1 (Martin et al. 2020b). The translocation breakpoint was localized in the pericentromeric region for chromosome 7, which explains the central position of chromosome 1 markers in LG1_7.

Among the various detected QTLs, 12 seemed highly promising (Table 3), nine of which were confirmed in the meta-analysis, with a marked reduction in CI enabling us to research candidate genes. Among these nine QTLs, three corresponded to major consensus QTLs with R^2 values over 25.0% (pH^WQTL-PM1_7.1, DMC^WQTL-PM9.2, and PF^WQTL-G6). Moreover, these three QTLs were involved in three MQTLs linked to several quality traits, thus highlighting colocalization between QTLs for these distinct traits. Relationship between such traits were previously reported in other fruits such as peach (Quilot et al. 2005; Desnoues et al. 2016), apple (Liebhard et al. 2003; Kenis et al. 2008) or tomato (Chaïb et al. 2006; Saliba-Colombani et al. 2001). Finally, two additional notable QTLs with R^2 values higher than 15.0%, were detected but only from the first approach, they concerned DMC^WQTL-PM9.1 and PF^WQTL-PM11. The latter was detected in particular at the end of fruit ripening. The tenth QTL with an R^2 close to 15.0%, which was not identified in the meta-analysis, was detected throughout the fruit ripening period (pH^WQTL-G6). We presume that this difference in QTL detection between the two approaches was related to the number of phenotyping data, which was higher in the first approach, thereby facilitating QTL detection. The variation in QTLs identified between production cycles in the second approach could be related to the different environmental

418 conditions. The impacts of climatic conditions—which could vary between crop cycles—are well-documented for
419 organoleptic fruit quality in banana (Peacock 1980; Daniells et al. 1992; Ambuko et al. 2006; Abd el Moniem et al.
420 2008; Hailu et al. 2013), as well as for other fruit such as tomato (Guichard et al. 2001; Mulholland et al. 2003;
421 Panthee et al. 2012) and melon (Bernillon et al. 2013). In addition to environmental effects, this difference could at
422 least partly be explained by the fact that in each cycle not all the same progeny individuals were phenotyped and the
423 number of progeny individuals phenotyped per cycle varied. Accordingly, QTLs detected in cycle 3, which involved
424 the lowest number of individuals, should be regarded with caution since the number of QTLs detected was reported
425 to increase as the population size decreased (Vales et al., 2005).
426
427 *4.2. Genetic control of banana quality traits*

428 Flavor, including taste and aroma, is the first quality perception criterion for consumer acceptance. Flavor
429 mainly depends on sugar and acid contents, and particularly on the sugar/acid ratio, which plays a role in both
430 sourness and sweetness perception (Bugaud et al. 2011, 2016). The majority of pH QTLs were detected on the
431 Pisang Madu genetic map, using both the whole dataset and per-cycle data. The increase in pH at the end of fruit
432 ripening, as observed in Pisang Madu, has been related to the decrease in acid contents, and described in banana
433 cultivars with low citrate levels and sometimes with high malate levels (Etienne et al. 2013a, 2014). The pH profile
434 observed for cv Galeo was typical of these acidic bananas and could be associated with high citrate contents (Etienne
435 et al., 2014). pH^{W}QTL-PM1_7.1 had the highest estimated effect for QTLs detected at the optimal maturity stage,
436 with R^2 values of 50.6 and 44.0% at days 6 and 7, respectively. The effects of additional pH QTLs were relatively
437 lower with, however, some pH QTLs having marked effects, especially during the first part of ripening on LG3
438 (pH^{W}QTL-PM3: 9.0%) and LG6 (pH^{W}QTL-G6: 5.6 to 14.4%).

439 Genes coding for enzymes involved in acid metabolism were found in the confidence interval of QTLs for
440 pH. They corresponded especially to the tricarboxylic acid cycle, namely with Aco, GAD, Mal, POX, PEPC and
441 PEPCK. A previous modelling study on banana acidity highlighted the potential role of NAD-malic enzyme and
442 mitochondrial malate carriers in the genotypic variability of citrate concentration differences (Etienne et al. 2014,
443 2015).These genes were linked to QTLs related to organic acid variations in other fruits like tomato (Causse et al.
444 2004), apple (Ban and Xu, 2020) and grappeberries (Chen et al., 2015). For malic acid variations among cultivars, a
445 similar approach highlighted the importance of proton pump activity and especially the free energy of ATP

hydrolysis (Etienne et al. 2014). This activity could be studied in relation to the pH MQTL-PM3.2, where gene coding to V-ATPase was detected. QTL regions with these genes were reported to influence malate accumulation in other fruits such as apple (Jia et al. 2018) and tomato (Causse et al. 2004).

After flavor, fruit texture—which can be assessed by pulp firmness—is the first consumer quality perception criterion for bananas (Bugaud et al. 2013). In addition, texture is essential for consumers with regard to shelflife and transportability (Bugaud et al. 2013; Jaiswal et al. 2014). The detected genetic effect of pulp firmness in the studied progeny was particularly low compared to other traits (PVE 12.2% and H^2 0,46), while presenting the highest interaction effects and residuals (PVE ~ 40.0%), which could be attributed to high variability between analytical replicates and a greater environmental influence on this trait compared to others. According to several studies on banana, fruit firmness depends on several factors, such as genotype (Saliba-Colombani et al. 2001), growth conditions (Ambuko et al. 2006; Bugaud et al. 2009), maturity stage at harvest and postharvest conditions (Ambuko et al. 2006; Salvador et al. 2007; Bugaud et al. 2007). Some cycle-specific QTLs were detected from the first two cycles, during the second part of ripening, close to the optimum stage of consumption. PF^{C1}QTL.G1 and PF^{C1}QTL.PM10 were both found at days 6 and 7, and PF^{C2}QTL.PM8 and PF^{C2}QTL.PM1_7.2 were detected on 4 different days from days 5 to 7. Several genes involved in cell wall metabolism were found in QTL intervals related to PF on the two maps, i.e. PF^{W}QTL-PM3 and PF^{W}QTL-G6. Genes involved in the auxin response and auxin signaling pathway that could regulate cell wall metabolism and influence fruit softening (Kumar et al. 2014) have been identified with PF^{W}QTL-PM4 and PF^{W}QTL-G4 within 0.9 Mb and 4.7 Mb, respectively. In tomato, through the SlARF4 gene, auxin has been found to control fruit firmness by regulating the pectin structure and tissue architecture (Jones et al. 2002; Sagar et al. 2013). Moreover, genes involved in the ethylene response (ETR) were found within the 1.5 Mb interval of PF^{W}QTL-G11. Ethylene and its biosynthetic genes have been implicated in fruit softening and shelflife maintenance regulation in several fleshy fruits (Xiong et al. 2005; Nishiyama et al. 2007; López-Gómez et al. 2009), e.g. via the expression of cell wall-related genes in tomato (Bu et al. 2013) apple (Wei et al. 2010), and peach (Hayama et al. 2006).

DMC is an important determinant with regard to several aspects of fruit quality such as fruit texture, including fruit firmness, storage and taste (Ferris et al. 1999; Bugaud et al. 2007). Bananas with higher pulp DMC

have thus been related to firm bananas and consumers have shown a preference for fruit with higher DMC, including plantain and cooking bananas at the green stage (Ferris et al. 1999; Gibert et al. 2009; Bugaud et al. 2013).

DMC presented high genetic determinism in the studied progeny (61.3% PVE), thus confirming the potential of this trait for dessert and cooking banana breeding schemes. In addition, DMC measured at harvest was correlated with DMC at the optimal stage ($r = 0.72$; data not shown). The high stability of DMC at the end of fruit growth and ripening had been pointed out in previous studies on banana (Ferris et al. 1999; Yomeni et al. 2004; Bugaud et al. 2007, 2012; Gibert et al. 2010) and mango (Lechaudel et al. 2005). This relationship prevails especially in climacteric fruit, like bananas, that accumulate starch during growth, which is converted into soluble sugars during ripening (Xiao et al. 2018). Consequently, although DMC was measured at three days of fruit ripening (days 1, 3 and 7), a significant number of QTLs were detected in the whole dataset. Among the QTLs associated with very low confidence intervals, most were detected for DMC, including those on LG9 (DMC^{W}QTL-PM9.1 and -PM9.2) and LG10 (DMC^{W}QTL-PM10 and -G10). Other QTLs detected presented high confidence intervals of over 19.0 Mb, which would hamper molecular breeding tool development. About 30.0% of DMC is attributed to structural dry mass, and cell walls (Etienne et al., 2014), which could explain why genes involved in cell wall dynamics colocalized with four DMC QTLs, including two MQTL (MQTL-PM8.1 and -PM11.2). Interestingly, genes related to several hormone metabolisms, such as auxin transport, ethylene response and gibberellin, colocalized with MQTL-PM11.2 within a 2.9 Mb region. This clustering of genes involved in the fruit development and growth phase may have a similar effect on the structural and non-structural dry matter content.

Several QTL colocalizations were identified for different quality traits on the two parent maps, suggesting physiological relationships between them. The closest correlations between pH and firmness values were observed during the first part of fruit ripening when these traits showed a concomitant decrease. The high number of QTL colocalizations observed for pH and PF could hence be explained by the links between ripening-related changes in pH and fruit texture. Several studies have suggested that changes in pH and mineral composition during fruit ripening may regulate cell wall hydrolase activity (Almeida and Huber 1999; Prasanna et al., 2007). The pH acidification trend during ripening has been found to be involved in fruit softening of several species (Johnston et al., 2002).

501 The colocalization between pH and DMC was expected as acids are major dry matter components. Frequent
502 colocalizations have been previously observed between QTLs for pulp dry matter and acidity in tomato (Paterson et
503 al. 1991; Saliba-Colombani et al. 2001) and peach (Dirlewanger et al. 1999). In such cases, it is difficult to
504 distinguish the pleiotropic effect of a single gene from the effects of the nearest genes.
505 The colocalization between PF and DMC could be explained by the hydrolysis of starch, i.e. the main DMC
506 compound, into soluble sugars during banana ripening (Bhuiyan et al., 2020). This causes an increase in osmotic
507 pressure and involves a decrease in turgor pressure associated with softening, as observed during berry (Thomas et
508 al., 2008) and tomato ripening (Saladié et al., 2007). Moreover, the pulp dry mass can be assessed by the sum of the
509 dry weights of the main non-structural compounds, such as soluble sugars, starch and acids, and the structural
510 compounds (Etienne et al, 2014), i.e. the constitutive part of pulp cells. This relationship between the structural dry
511 matter component and cell walls could explain the indirect links between DMC and PF.
512 Finally, we also noted significant QTL clustering, including a large cluster containing QTLs for all
513 measured traits localized on LG10. This clustering may be due to tight linkage between QTLs (clustering of different
514 genes) and/or may indicate the presence of a single QTL with pleiotropic effects. Similar fruit quality QTL clusters
515 have been reported in other fruit species, including peach (Quilot et al. 2005; Desnoues et al. 2016), apple (Liebhard
516 et al. 2003; Kenis et al. 2008) and tomato (Chaïb et al. 2006).
517
518 **5. Conclusion**
519 High heritability was found in the progeny for the three studied traits, although pulp firmness seemed to be
520 more affected by environmental factors. Breeding and prebreeding approaches should thus permit to improve these
521 characters.
522 Several promising QTLs (R^2 >15.0%) were detected for the three characters, including three major QTLs
523 (R^2 > 25.0%) –one per trait- (pH^WQTL-PM1_7.1, DMC^WQTL-PM9.2, and PF^WQTL-G6). They should now be
524 validated in other genetic contexts and their confidence intervals would need to be refined before envisioning MAS
525 selection.
526 One particularly interesting QTL is QTL pH^WQTL-PM1_7.1 that had the highest estimated effect at the
527 optimal maturity stage, with an R^2 of 50.6 and 44.0% at days 6 and 7, respectively. We showed that the
528 corresponding haplotype in chromosome 1T7 of Pisang Madu was associated with higher pH at fruit maturity, which

529 is a sweet dessert banana characteristic. This haplotype in Pisang Madu is located, in a region of Chr 1T7 that does
530 not recombine in this heterozygous context and corresponds to reference chromosome 1. This could thus be an
531 advantage for MAS, since selection for this QTL could be performed using any specific markers from chromosome 1
532 in this progeny and potentially in other progeny of parents structurally heterozygous for the 1T7 chromosome
533 structure. The effects of this QTL in other genomic contexts have yet to be tested, but could potentially explain the
534 success of the 1T7 chromosomal structure to which it is associated and which has been found in many dessert
535 cultivars including Cavendish, that accounts for 50.0% of world banana production (Martin et al., 2020b).
536
537
538 **Acknowledgements**
539 We are grateful to all the staff members of the CIRAD's banana breeding platform in Guadeloupe who were
540 involved in the progeny development, growing and phenotyping. We thank Dr Lucile Toniutti and Dr David Pot for
541 critically reading the manuscript.The CIRAD – UMR AGAP HPC Data Center of the South Green Bioinformatics
542 platform (http://www.southgreen.fr) provided the computational resources.
543
544 **Author Contribution**
545 **Stella Biabiany**: Investigation, Formal analysis, Writing - Original Draft ; **Emilie Araou**: Resources, Methodology,
546 Investigation ; **Fabien Cormier**: Methodology, Validation; **Guillaume Martin**: Software, Data curation, Formal
547 analysis, Writing – review and editing; **Françoise Carreel**: Methodology, Validation; **Catherine Hervouet**:
548 Resources; **Frédéric Salmon**: Methodology, Resources; **Jean-Claude Efile**: Methodology, Resources; **Felicie**
549 **Lopez-Lauri**: Supervision; **Angélique D'Hont**: Supervision, Writing - Original Draft; **Mathieu Léchaudel**:
550 Conceptualization, Methodology, Formal analysis, Supervision, Writing - Original Draft, **Sébastien Ricci**:
551 Conceptualization, Methodology, Resources, Supervision, Writing - Original Draft.
552
553 **Funding**
554 This work was supported by CIRAD, the European Agricultural Fund for Rural Development (EAFRD) 'Plan
555 Banane Durable 2' program, the France Genomique programme (ANR-10-INBS-09-08) 'DynaMo' project with
556 Genoscope/CEA, the French Investissements d'avenir programme (Labex Agro: ANR- 10-LABX-0001-01)

Agropolis Fondation (ID 1504-006) 'GenomeHarvest', and the CGIAR Research Programme on Roots, Tubers and Bananas

Declaration of Competing Interest

The authors declare that they have no conflict of interest.

Availability of data and material

The data that support the findings of this study are available from the authors upon request.

References

Abd el Moniem EA, A. S. E. Abd-Allah, Ahmed MA (2008) The combined effect of some organic manures, mineral N fertilizers and algal cells extract on yield and fruit quality of Williams banana plants. Agric & Environ Sci 4:417-426

Ahmad F, Martawi NM, Poerba YS, de Jong H, Schouten H, Kema GH (2020) Genetic mapping of Fusarium wilt resistance in a wild banana Musa acuminata ssp. malaccensis accession. Theoretical and Applied Genetics 133:3409-3418

Akaike H (1974) A new look at the statistical model identification. IEEE Transactions on Automatic Control 19:716-723

Almeida DPF, Huber DJ (1999) Apoplastic pH and inorganic ion levels in tomato fruit: A potential means for regulation of cell wall metabolism during ripening. Physiologia Plantarum 105:506-512

Ambuko JL, Sekozawa Y, Sugaya S, Itoh F, Nakamura K, Gemma H (2006) EFFECT OF SEASONAL VARIATION, CULTIVAR AND PRODUCTION SYSTEM ON SOME POSTHARVEST CHARACTERISTICS OF THE BANANA. 712 edn. International Society for Horticultural Science (ISHS), Leuven, Belgium, pp 505-510

Arcade A, Labourdette A, Falque M, Mangin B, Chardon F, Charcosset A, Joets J (2004) BioMercator: integrating genetic maps and QTL towards discovery of candidate genes. Bioinformatics 20:2324-2326

Arends D, Prins P, Jansen RC, Broman KW (2010) R/qtl: high-throughput multiple QTL mapping. Bioinformatics 26:2990-2992

Bakry F (2008) Zygotic embryo rescue in bananas. Fruits 63:111-115

Bakry F, Carreel F, Jenny C, Horry J-P (2009) Genetic improvement of banana. Breeding plantation tree crops: tropical species. Springer, pp 3-50

Baurens F-C, Martin G, Hervouet C, Salmon F, Yohomé D, Ricci S, Rouard M, Habas R, Lemainque A, Yahiaoui N (2019) Recombination and large structural variations shape interspecific edible bananas genomes. Molecular biology and evolution 36:97-111

Bernillon S, Biais B, Deborde C, Maucourt M, Cabasson C, Gibon Y, Hansen TH, Husted S, de Vos RCH, Mumm R, Jonker H, Ward JL, Miller SJ, Baker JM, Burger J, Tadmor Ya, Beale MH, Schjoerring JK, Schaffer AA, Rolin D, Hall RD, Moing A (2013) Metabolomic and elemental profiling of melon fruit quality as affected by genotype and environment. Metabolomics 9:57-77

Bhuiyan F, Campos NA, Swennen R, Carpentier S (2020) Characterizing fruit ripening in plantain and Cavendish bananas: A proteomics approach. Journal of Proteomics 214:103632

Broman KW, Sen S (2009) A Guide to QTL Mapping with R/qtl. New York: Springer

593 Bu J, Yu Y, Aisikaer G, Ying T (2013) Postharvest UV-C irradiation inhibits the production of ethylene and the activity of cell wall-
594 degrading enzymes during softening of tomato (Lycopersicon esculentum L.) fruit. Postharvest Biology and Technology 86:337-
595 345

596 Bugaud C, Belleil T, Daribo M-O, Génard M (2012) Does bunch trimming affect dry matter content in banana? Scientia
597 Horticulturae 144:125-129

598 Bugaud C, Cazevieille P, Daribo M-O, Telle N, Julianus P, Fils-Lycaon B, Mbéguié-A-Mbéguié D (2013) Rheological and chemical
599 predictors of texture and taste in dessert banana (Musa spp.). Postharvest Biology and Technology 84:1-8

600 Bugaud C, Daribo MO, Dubois C (2007) Climatic conditions affect the texture and colour of Cavendish bananas (Grande Naine
601 cultivar). Scientia Horticulturae 113:238-243

602 Bugaud C, Daribo M-O, Beauté M-P, Telle N, Dubois C (2009) Relative importance of location and period of banana bunch
603 growth in carbohydrate content and mineral composition of fruit. Fruits 64:63-74

604 Bugaud C, Deverge E, Daribo MO, Ribeyre F, Fils-Lycaon B, Mbéguié-A-Mbéguié D (2011) Sensory characterisation enabled the
605 first classification of dessert bananas. Journal of the Science of Food and Agriculture 91:992-1000

606 Bugaud C, Maraval I, Daribo M-O, Leclerc N, Salmon F (2016) Optimal and acceptable levels of sweetness, sourness, firmness,
607 mealiness and banana aroma in dessert banana (Musa sp.). Scientia Horticulturae 211:399-409

608 Carreel F, De Leon DG, Lagoda P, Lanaud C, Jenny C, Horry J-P, Du Montcel HT (2002) Ascertaining maternal and paternal lineage
609 within Musa by chloroplast and mitochondrial DNA RFLP analyses. Genome 45:679-692

610 Causse M, Duffe P, Gomez MC, Buret M, Damidaux R, Zamir D, Gur A, Chevalier C, Lemaire-Chamley M, Rothan C (2004) A
611 genetic map of candidate genes and QTLs involved in tomato fruit size and composition. Journal of Experimental Botany
612 55:1671-1685

613 Causse M, Saliba-Colombani V, Lecomte L, Duffé P, Rousselle P, Buret M (2002) QTL analysis of fruit quality in fresh market
614 tomato: a few chromosome regions control the variation of sensory and instrumental traits. Journal of Experimental Botany
615 53:2089-2098

616 Causse M, Saliba-Colombani V, Lesschaeve I, Buret M (2001) Genetic analysis of organoleptic quality in fresh market tomato. 2.
617 Mapping QTLs for sensory attributes. Theoretical and Applied Genetics 102:273-283

618 Cenci A, Sardos J, Hueber Y, Martin G, Breton C, Roux N, Swennen R, Carpentier SC, Rouard M (2020) Unravelling the complex
619 story of intergenomic recombination in ABB allotriploid bananas. Annals of Botany 127:7-20

620 Chaïb J (2006) Stability over genetic backgrounds, generations and years of quantitative trait locus (QTLs) for organoleptic
621 quality in tomato. Theoretical and applied genetics v. 112:pp. 934-944-2006 v.2112 no.2005

622 Chillet M, de Lapeyre de Bellaire L, Hubert O, Mbéguié-A-Mbéguié D (2008) Mechanical characterisation of banana fruits. Fruits
623 63:51-52

624 Christelová P, Valárik M, Hřibová E, Van den houwe I, Channelière S, Roux N, Doležel J (2011) A platform for efficient genotyping
625 in Musa using microsatellite markers. AoB PLANTS 2011

626 Costa F, Peace CP, Stella S, Serra S, Musacchi S, Bazzani M, Sansavini S, Van de Weg WE (2010) QTL dynamics for fruit firmness
627 and softening around an ethylene-dependent polygalacturonase gene in apple (Malus×domestica Borkh.). Journal of
628 Experimental Botany 61:3029-3039

629 Cullis BR, Smith AB, Coombes NE (2006) On the design of early generation variety trials with correlated data. Journal of
630 Agricultural, Biological, and Environmental Statistics 11:381

631 D'hont A, Denoeud F, Aury J-M, Baurens F-C, Carreel F, Garsmeur O, Noel B, Bocs S, Droc G, Rouard M (2012) The banana (Musa
632 acuminata) genome and the evolution of monocotyledonous plants. Nature 488:213-217

633 Daniells J, Lisle A, O'Farrell P (1992) Effect of bunch-covering methods on maturity bronzing, yield, and fruit quality of bananas in
634 North Queensland. Australian Journal of Experimental Agriculture 32:121-125

635 Desnoues E, Baldazzi V, Génard M, Mauroux J-B, Lambert P, Confolent C, Quilot-Turion B (2016) Dynamic QTLs for sugars and
636 enzyme activities provide an overview of genetic control of sugar metabolism during peach fruit development. Journal of
637 Experimental Botany 67:3419-3431

638 Dirlewanger E, Moing A, Rothan C, Svanella L, Pronier V, Guye A, Plomion C, Monet R (1999) Mapping QTLs controlling fruit
639 quality in peach (Prunus persica (L.) Batsch). Theoretical and Applied Genetics 98:18-31

640 DOLEŽEL J, BARTOŠ J (2005) Plant DNA Flow Cytometry and Estimation of Nuclear Genome Size. Annals of Botany 95:99-110

641 Dolezel J, Binarovk P, Lucretti S (1989) Analysis of nuclear DNA content in plant cells by flow

642 cytometry. Biol Plant 31:113-120

643 Dupouy M, Baurens F-C, Derouault P, Hervouet C, Cardi C, Cruaud C, Istace B, Labadie K, Guiougou C, Toubi L (2019) Two large
644 reciprocal translocations characterized in the disease resistance-rich burmannica genetic group of Musa acuminata. Annals of
645 botany 124:319-329

646 Etienne A, Génard M, Bancel D, Benoit S, Bugaud C (2013a) A model approach revealed the relationship between banana pulp
647 acidity and composition during growth and post harvest ripening. Scientia Horticulturae 162:125-134

648 Etienne A, Génard M, Bancel D, Benoit S, Lemire G, Bugaud C (2014) Citrate and malate accumulation in banana fruit (Musa sp.
649 AA) is highly affected by genotype and fruit age, but not by cultural practices. Scientia Horticulturae 169:99-110

650 Etienne A, Génard M, Bugaud C (2015) A process-based model of TCA cycle functioning to analyze citrate accumulation in pre-
651 and post-harvest fruits. PloS one 10:e0126777

652 Etienne A, Génard M, Lobit P, Mbeguié-A-Mbéguié D, Bugaud C (2013b) What controls fleshy fruit acidity? A review of malate
653 and citrate accumulation in fruit cells. Journal of experimental botany 64:1451-1469

654 Fauré S, Noyer J-L, Horry J-P, Bakry F, Lanaud C, de León DG (1993) A molecular marker-based linkage map of diploid bananas
655 (Musa acuminata). Theoretical and Applied Genetics 87:517-526

656 Garsmeur O, Droc G, Antonise R, Grimwood J, Potier B, Aitken K, Jenkins J, Martin G, Charron C, Hervouet C, Costet L, Yahiaoui
657 N, Healey A, Sims D, Cherukuri Y, Sreedasyam A, Kilian A, Chan A, Van Sluys M-A, Swaminathan K, Town C, Bergès H, Simmons B,
658 Glaszmann JC, van der Vossen E, Henry R, Schmutz J, D'Hont A (2018) A mosaic monoploid reference sequence for the highly
659 complex genome of sugarcane. Nature Communications 9:2638

660 Gibert C, Génard M, Vercambre G, Lescourret F (2010) Quantification and modelling of the stomatal, cuticular and crack
661 components of peach fruit surface conductance. Functional Plant Biology 37:264-274

662 Gibert O, Dufour D, Giraldo A, Sanchez T, Reynes M, Pain J-P, Gonzalez A, Fernandez A, Diaz A (2009) Differentiation between
663 cooking bananas and dessert bananas. 1. Morphological and compositional characterization of cultivated Colombian Musaceae
664 (Musa sp.) in relation to consumer preferences. Journal of Agricultural and Food Chemistry 57:7857-7869

665 Guichard S, Bertin N, Leonardi C, Gary C (2001) Tomato fruit quality in relation to water and carbon fluxes. Agronomie 21:385-
666 392

667 Hailu M, Tilahun Seyoum Workneh, Belew D (2013) Review on postharvest technology of banana fruit. African Journal of
668 Biotechnology 12

669 Hayama H, Shimada T, Fujii H, Ito A, Kashimura Y (2006) Ethylene-regulation of fruit softening and softening-related genes in
670 peach. Journal of Experimental Botany 57:4071-4077

671 Henderson CR (1950) Estimation of genetic parameters. Ann Math Stat 21:309

672 Herten K, Hestand MS, Vermeesch JR, Van Houdt JKJ (2015) GBSX: a toolkit for experimental design and demultiplexing
673 genotyping by sequencing experiments. BMC Bioinformatics 16:73

674 Hippolyte I, Bakry F, Seguin M, Gardes L, Rivallan R, Risterucci A-M, Jenny C, Perrier X, Carreel F, Argout X (2010) A saturated
675 SSR/DArT linkage map of Musa acuminata addressing genome rearrangements among bananas. BMC plant biology 10:1-18

Hubert O, Piral G, Galas C, Baurens F-C, Mbéguié-A-Mbéguié D (2014) Changes in ethylene signaling and MADS box gene expression are associated with banana finger drop. Plant Science 223:99-108

Jaiswal P, Jha SN, Kaur PP, Bhardwaj R, Singh AK, Wadhawan V (2014) Prediction of textural attributes using color values of banana (Musa sapientum) during ripening. Journal of Food Science and Technology 51:1179-1184

Jia D, Shen F, Wang Y, Wu T, Xu X, Zhang X, Han Z (2018) Apple fruit acidity is genetically diversified by natural variations in three hierarchical epistatic genes: MdSAUR37, MdPP2CH and MdALMTII. The Plant Journal 95:427-443

Johnston JW, Hewett EW, Hertog MLATM (2002) Postharvest softening of apple (Malus domestica) fruit: A review. New Zealand Journal of Crop and Horticultural Science 30:145-160

Jones B, Frasse P, Olmos E, Zegzouti H, Li ZG, Latché A, Pech JC, Bouzayen M (2002) Down-regulation of DR12, an auxin-response-factor homolog, in the tomato results in a pleiotropic phenotype including dark green and blotchy ripening fruit. The Plant Journal 32:603-613

Kenis K, Keulemans J, Davey MW (2008) Identification and stability of QTLs for fruit quality traits in apple. Tree Genetics & Genomes 4:647-661

Kosambi DD (2016) The Estimation of Map Distances from Recombination Values. In: Ramaswamy R (ed) DD Kosambi: Selected Works in Mathematics and Statistics. Springer India, New Delhi, pp 125-130

Kouassi HA, Assemand EF, Gibert O, Maraval I, Ricci J, Thiemele DEF, Bugaud C (2021) Textural and physicochemical predictors of sensory texture and sweetness of boiled plantain. International Journal of Food Science & Technology 56:1160-1170

Kumar R, Khurana A, Sharma AK (2014) Role of plant hormones and their interplay in development and ripening of fleshy fruits. Journal of Experimental Botany 65:4561-4575

Lagoda PJL, Dambier D, Grapin A, Baurens F-C, Lanaud C, Noyer J-L (1998) Nonradioactive sequence-tagged microsatellite site analyses: A method transferable to the tropics. ELECTROPHORESIS 19:152-157

Léchaudel M, Génard M, Lescourret F, Urban L, Jannoyer M (2005) Modeling effects of weather and source–sink relationships on mango fruit growth. Tree Physiology 25:583-597

Lescot T (2020) Banana genetic diversity. Fruitrop 269:98-102

Liebhard R, Kellerhals M, Pfammatter W, Jertmini M, Gessler C (2003) Mapping quantitative physiological traits in apple (Malus × domestica Borkh.). Plant Molecular Biology 52:511-526

López-Gómez R, Cabrera-Ponce JL, Saucedo-Arias LJ, Carreto-Montoya L, Villanueva-Arce R, Díaz-Perez JC, Gómez-Lim MA, Herrera-Estrella L (2009) Ripening in papaya fruit is altered by ACC oxidase cosuppression. Transgenic research 18:89-97

Martin G, Baurens Fc, Hervouet C, Salmon F, Delos Jm, Labadie K, Perdereau A, Mournet P, Blois L, Dupouy M (2020b) Chromosome reciprocal translocations have accompanied subspecies evolution in bananas. The Plant Journal 104:1698-1711

Martin G, Baurens F-C, Droc G, Rouard M, Cenci A, Kilian A, Hastie A, Doležel J, Aury J-M, Alberti A, Carreel F, D'Hont A (2016) Improvement of the banana "Musa acuminata" reference sequence using NGS data and semi-automated bioinformatics methods. BMC Genomics 17:243

Martin G, Cardi C, Sarah G, Ricci S, Jenny C, Fondi E, Perrier X, Glaszmann JC, d'Hont A, Yahiaoui N (2020a) Genome ancestry mosaics reveal multiple and cryptic contributors to cultivated banana. The Plant Journal 102:1008-1025

Martin G, Carreel F, Coriton O, Hervouet C, Cardi C, Derouault P, Roques D, Salmon F, Rouard M, Sardos J (2017) Evolution of the banana genome (Musa acuminata) is impacted by large chromosomal translocations. Molecular biology and evolution 34:2140-2152

Martin M (2011) Cutadapt removes adapter sequences from high-throughput sequencing reads. 2011 17:3

Mbanjo EGN, Tchoumbougnang F, Mouelle AS, Oben JE, Nyine M, Dochez C, Ferguson ME, Lorenzen J (2012) Molecular marker-based genetic linkage map of a diploid banana population (Musa acuminata Colla). Euphytica 188:369-386

Mulholland BJ, Edmondson RN, Fussell M, Basham J, Ho LC (2003) Effects of high temperature on tomato summer fruit quality. The Journal of Horticultural Science and Biotechnology 78:365-374

Nishiyama K, Guis M, Rose JKC, Kubo Y, Bennett KA, Wangjin L, Kato K, Ushijima K, Nakano R, Inaba A, Bouzayen M, Latche A, Pech J-C, Bennett AB (2007) Ethylene regulation of fruit softening and cell wall disassembly in Charentais melon. Journal of Experimental Botany 58:1281-1290

Noumbissié G, Chabannes M, Bakry F, Ricci S, Cardi C, Njembele J-C, Yohoume D, Tomekpe K, Iskra-Caruana M-L, d'Hont A (2016) Chromosome segregation in an allotetraploid banana hybrid (AAAB) suggests a translocation between the A and B genomes and results in eBSV-free offsprings. Molecular Breeding 36:38

Nyine M, Uwimana B, Akech V, Brown A, Ortiz R, Doležel J, Lorenzen J, Swennen R (2019) Association genetics of bunch weight and its component traits in East African highland banana (Musa spp. AAA group). Theoretical and Applied Genetics 132:3295-3308

Panthee DR, Cao C, Debenport SJ, Rodríguez GR, Labate JA, Robertson LD, Breksa AP, van der Knaap E, McSpadden Gardener BB (2012) Magnitude of Genotype × Environment Interactions Affecting Tomato Fruit Quality. HortScience horts 47:721-726

Paterson AH, Damon S, Hewitt JD, Zamir D, Rabinowitch HD, Lincoln SE, Lander ES, Tanksley SD (1991) Mendelian factors underlying quantitative traits in tomato: comparison across species, generations, and environments. Genetics 127:181-197

Peacock BC (1980) Banana ripening: effect of temperature on fruit quality. Queensland Journal of Agricultural and Animal Sciences (Australia) 37:39-45

Perrier X, Bakry F, Carreel F, Jenny C, Horry J-P, Lebot V, Hippolyte I (2009) Combining biological approaches to shed light on the evolution of edible bananas

Phillips KM, McGinty RC, Couture G, Pehrsson PR, McKillop K, Fukagawa NK (2021) Dietary fiber, starch, and sugars in bananas at different stages of ripeness in the retail market. PLoS ONE 16(7): e0253366

Prasanna V, Prabha TN, Tharanathan RN (2007) Fruit Ripening Phenomena–An Overview. Critical Reviews in Food Science and Nutrition 47:1-19

Quilot B, Kervella J, Génard M, Lescourret F (2005) Analysing the genetic control of peach fruit quality through an ecophysiological model combined with a QTL approach. Journal of Experimental Botany 56:3083-3092

Quinlan AR, Hall IM (2010) BEDTools: a flexible suite of utilities for comparing genomic features. Bioinformatics 26:841-842

Risterucci A-M, Grivet L, N'Goran JA, Pieretti I, Flament M-H, Lanaud C (2000) A high-density linkage map of Theobroma cacao L. Theoretical and Applied Genetics 101:948-955

Sagar M, Chervin C, Mila I, Hao Y, Roustan J-P, Benichou M, Gibon Y, Biais B, Maury P, Latché A, Pech J-C, Bouzayen M, Zouine M (2013) SlARF4, an Auxin Response Factor Involved in the Control of Sugar Metabolism during Tomato Fruit Development Plant Physiology 161:1362-1374

Saladié M, Matas AJ, Isaacson T, Jenks MA, Goodwin SM, Niklas KJ, Xiaolin R, Labavitch JM, Shackel KA, Fernie AR, Lytovchenko A, O'Neill MA, Watkins CB, Rose JKC (2007) A Reevaluation of the Key Factors That Influence Tomato Fruit Softening and Integrity. Plant Physiology 144:1012-1028

Saliba-Colombani V, Causse M, M., Langlois D, Philouze J, BURET M (2001) Genetic analysis of organoleptic quality in fresh market tomato. 1. Mapping QTLs for physical and chemical traits. TAG Theoretical and Applied Genetics 102:259-272

Salvador A, Sanz T, Fiszman SM (2007) Changes in colour and texture and their relationship with eating quality during storage of two different dessert bananas. Postharvest Biology and Technology 43:319-325

Sardos J, Rouard M, Hueber Y, Cenci A, Hyma KE, Van Den Houwe I, Hribova E, Courtois B, Roux N (2016) A genome-wide association study on the seedless phenotype in banana (Musa spp.) reveals the potential of a selected panel to detect candidate genes in a vegetatively propagated crop. PLoS One 11:e0154448

Shen Y, Xiang Y, Xu E, Ge X, Li Z (2018) Major Co-localized QTL for Plant Height, Branch Initiation Height, Stem Diameter, and Flowering Time in an Alien Introgression Derived Brassica napus DH Population. Frontiers in Plant Science 9

Šimoníková D, Němečková A, Čížková J, Brown A, Swennen R, Doležel J, Hřibová E (2020) Chromosome Painting in Cultivated Bananas and Their Wild Relatives (Musa spp.) Reveals Differences in Chromosome Structure. International journal of molecular sciences 21:7915

Sun YD, Liang Y, Wu JM, Li YZ, Cui X, Qin L (2012) Dynamic QTL analysis for fruit lycopene content and total soluble solid content in a Solanum lycopersicum x S. pimpinellifolium cross. Genetics and molecular research : GMR 11:3696-3710

Team RC (2020) R: A language and environment for statistical computing. . R Foundation for Statistical Computing, Vienna, Austria.

Thomas TR, Shackel KA, Matthews MA (2008) Mesocarp cell turgor in Vitis vinifera L. berries throughout development and its relation to firmness, growth, and the onset of ripening. Planta 228:1067

Vales MI, Schön CC, Capettini F, Chen XM, Corey AE, Mather DE, Mundt CC, Richardson KL, Sandoval-Islas JS, Utz HF, Hayes PM (2005) Effect of population size on the estimation of QTL: a test using resistance to barley stripe rust. Theor Appl Genet 111:1260-1270

Van Ooijen J (2006) JoinMap(R) 4, software for the calculation of genetic linkage maps in experimental population

Vázquez-Ovando A, Andrino-López D, Adriano-Anaya L, Miguel S, Ovando-Medina I (2012) Sensory and physico-chemical quality of banana fruits “Grand Naine” grown with biofertilizer. - African J Agricultural Research 7:4620-4626

Wakabayashi K (2000) Changes in Cell Wall Polysaccharides During Fruit Ripening. Journal of Plant Research 113:231-237

Wei J, Ma F, Shi S, Qi X, Zhu X, Yuan J (2010) Changes and postharvest regulation of activity and gene expression of enzymes related to cell wall degradation in ripening apple fruit. Postharvest Biology and Technology 56:147-154

Wu X-L, Hu Z-L (2012) Meta-analysis of QTL Mapping Experiments. In: Rifkin SA (ed) Quantitative Trait Loci (QTL): Methods and Protocols. Humana Press, Totowa, NJ, pp 145-171

Xiao Y-Y, Kuang J-F, Qi X-N, Ye Y-J, Wu Z-X, Chen J-Y, Lu W-J (2018) A comprehensive investigation of starch degradation process and identification of a transcriptional activator MabHLH6 during banana fruit ripening. Plant Biotechnol J 16:151-164

Xiong A-S, Yao Q-H, Peng R-H, Li X, Han P-L, Fan H-Q (2005) Different effects on ACC oxidase gene silencing triggered by RNA interference in transgenic tomato. Plant Cell Reports 23:639-646

Yomeni M, Njoukam J, Tchango Tchango J (2004) Influence of the stage of ripeness of plantains and some cooking bananas on the sensory and physicochemical characteristics of processed products. Journal of the Science of Food and Agriculture 84:1069-1077

Figure captions:

Fig. 1 Genetic map and QTL detected on LG 1_7. **a**: comparison of the genetic linkage map of LG1_7 with the physical map of reference chromosomes 1 and 7, **b**: location of the QTL related to the quality traits studied detected in the two approaches (W: whole dataset, C: production cycle datasets, with C1, C2 and C3 for cycles 1, 2 and 3, respectively) and the meta-analysis (MQTL), **c**: detail of QTLs for each day of the fruit ripening process that contributed to the two consensus pH QTLs identified in the first two approaches and confirmed by the meta-analysis , **d**: box plot representation of mean pH values at day 7 (corresponding to ripe fruit) of individuals with haplotype 1 (1/7 translocated chromosome structure) of Pisang Madu and individuals with haplotype 2 (reference chromosome structure) of Pisang Madu . Different letters indicate that haplotype averages are significantly different at $P<0.05$ (according to Tukey's multiple comparison test)

Fig. 2 Boxplots of pulp pH, firmness (PF, in N) and dry matter content (DMC, in %) measured at the various studied fruit ripening days for all progeny individuals, either at all production cycles (**a**, **e**, **i**), or at cycles 1 (**b**, **f**, **j**), 2 (**c**, **g**, **k**) and 3 (**d**, **h**, **l**)

Fig. 3 Number of QTLs detected for the three quality traits, i.e. pulp pH, firmness (PF, in N) and dry matter content (DMC, in %) on Pisang Madu (black) and Galeo (white) maps in the first QTL mapping approach on the whole dataset (**a**) and in the second approach on the three production cycle datasets (**b** and **c**) from Pisang Madu polymorphism (**b**) and Galeo polymorphism (**c**) for each cycle

Fig. 4 Physical map based on reference chromosomes (except 1 and 7) and QTLs detected in both QTL mapping approaches and the meta-analysis, and QTLs from the first approach (whole dataset) with an R^2 higher than 15%. QTLs are identified according to the quality trait, i.e. pulp pH (red), firmness (green) and dry matter content (blue, the dataset (W: whole dataset, C: production cycle datasets, with C1, C2 and C3 for cycles 1, 2 and 3, respectively) and the origin of linkage groups with Galeo (G) and Pisang Madu (PM). The location of SNP markers, QTLs, and MQTLs (grey) are indicated

Fig. 1

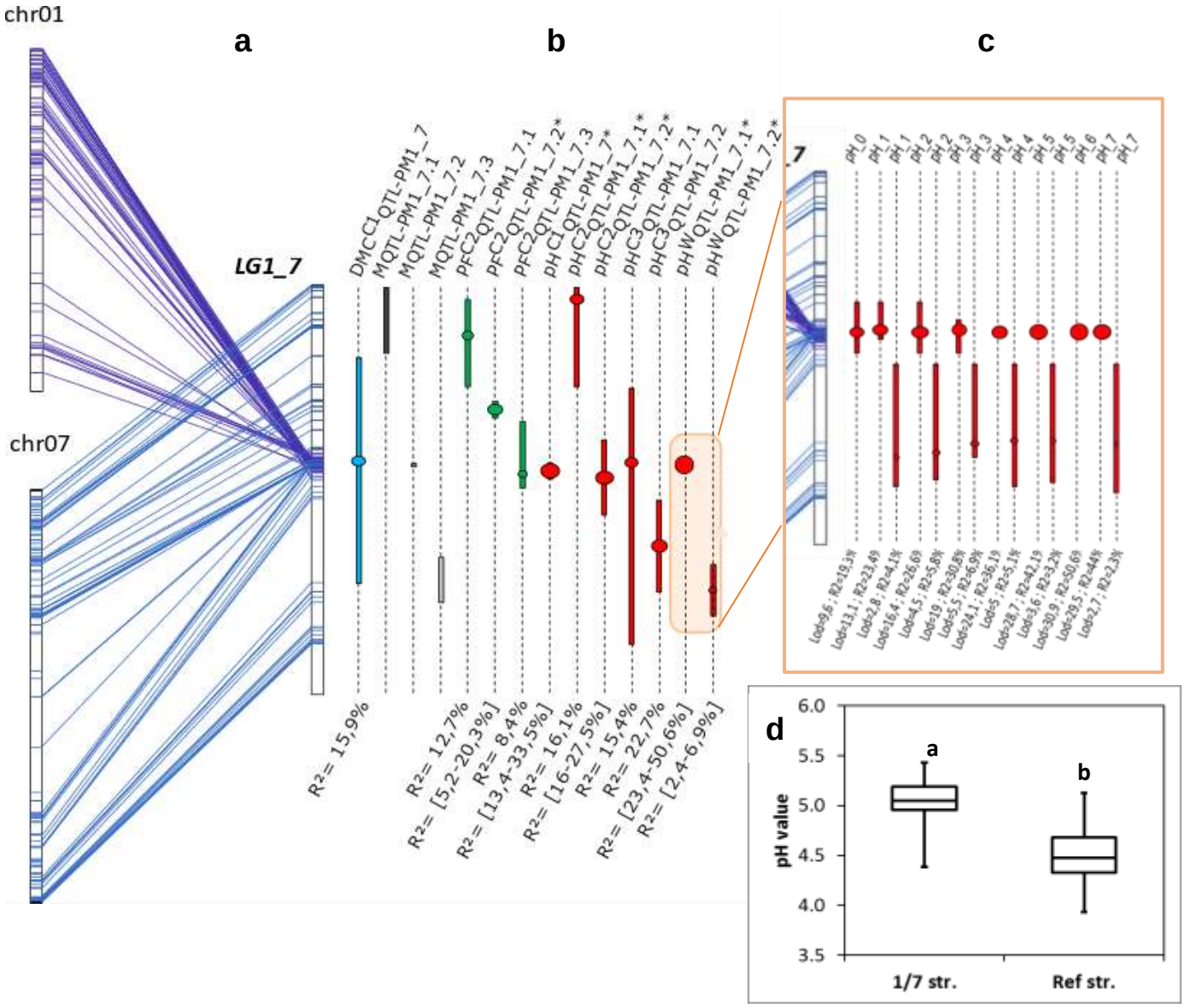
chr01
chr07
a
b
c
d
LG1_7
DMCC1QTL-PM1_7
MQTL-PM1_7.1
MQTL-PM1_7.2
MQTL-PM1_7.3
PFC2QTL-PM1_7.1
PFC2QTL-PM1_7.2*
pHC1QTL-PM1_7.3
pHC2QTL-PM1_7*
pHC2QTL-PM1_7.1*
pHC2QTL-PM1_7.2*
pHC3QTL-PM1_7.1
pHWQTL-PM1_7.2
pHWQTL-PM1_7.1*
pHWQTL-PM1_7.2*
R²= 15,9%
R²= 12,7%
R²= [5,2-20,3%]
R²= 8,4%
R²= [13,4-33,5%]
R²= 16,1%
R²= [16-27,5%]
R²= 15,4%
R²= 22,7%
R²= [23,4-50,6%]
R²= [2,4-6,9%]
pH value
6.0
5.5
5.0
4.5
4.0
3.5
a
b
1/7 str.
Ref str.

Fig. 2

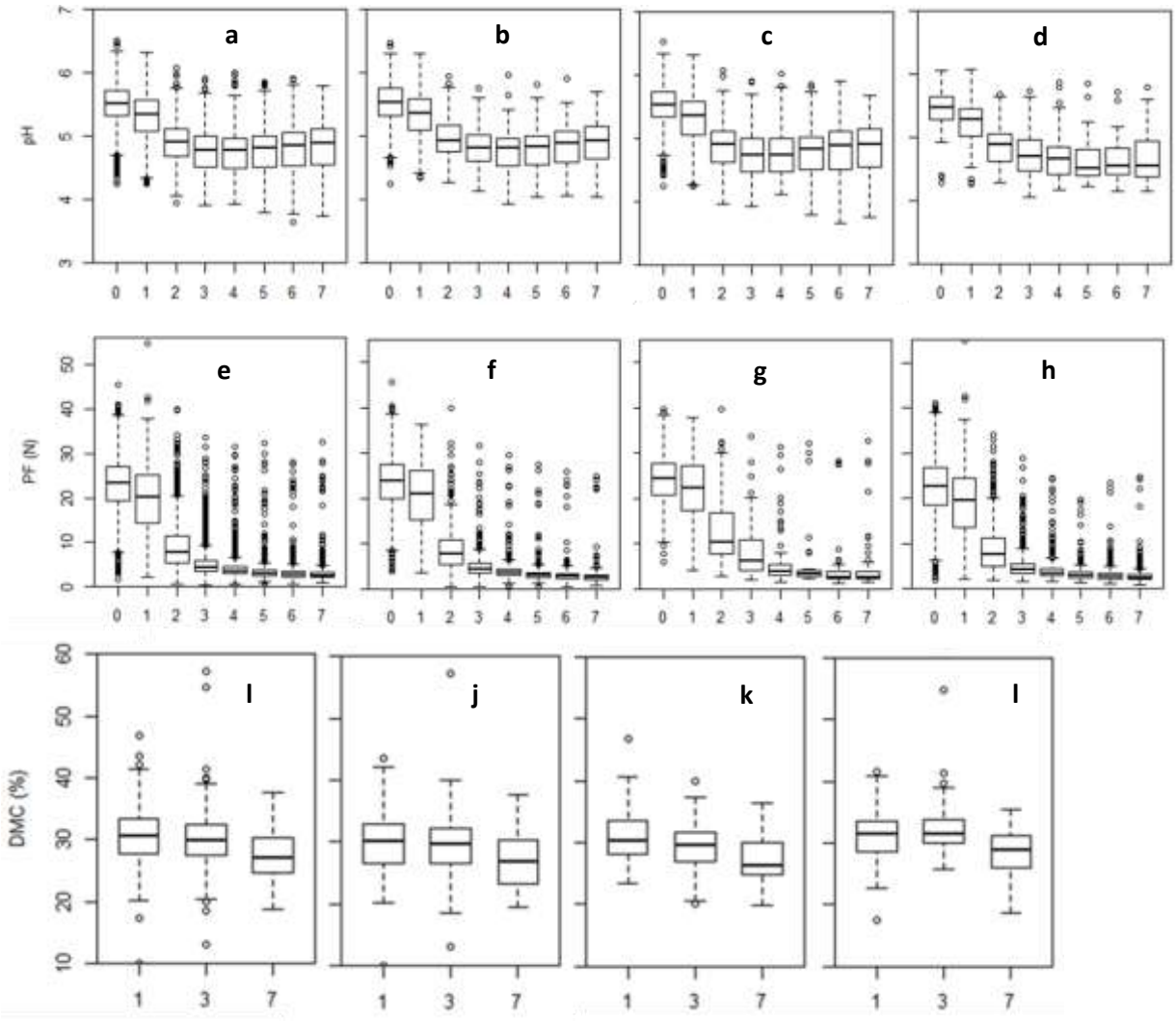

Fig. 3

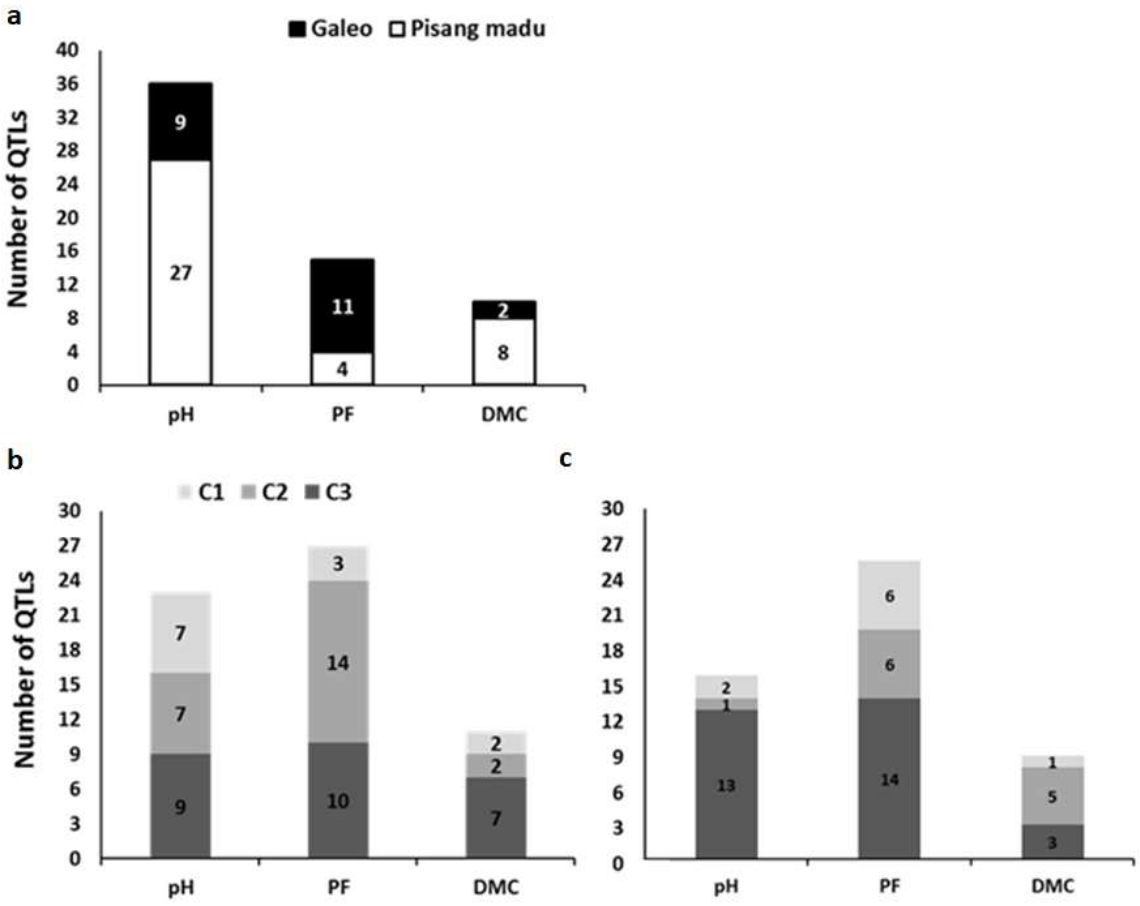
a
Galeo
Pisang madu
Number of QTLs
40
36
32
28
24
20
16
12
8
4
0
9
27
11
4
2
8
pH
PF
DMC
b
C1
C2
C3
Number of QTLs
30
27
24
21
18
15
12
9
6
3
0
7
7
9
3
14
10
2
2
7
pH
PF
DMC
c
30
27
24
21
18
15
12
9
6
3
0
2
1
13
6
6
14
1
5
3
pH
PF
DMC

Fig. 4

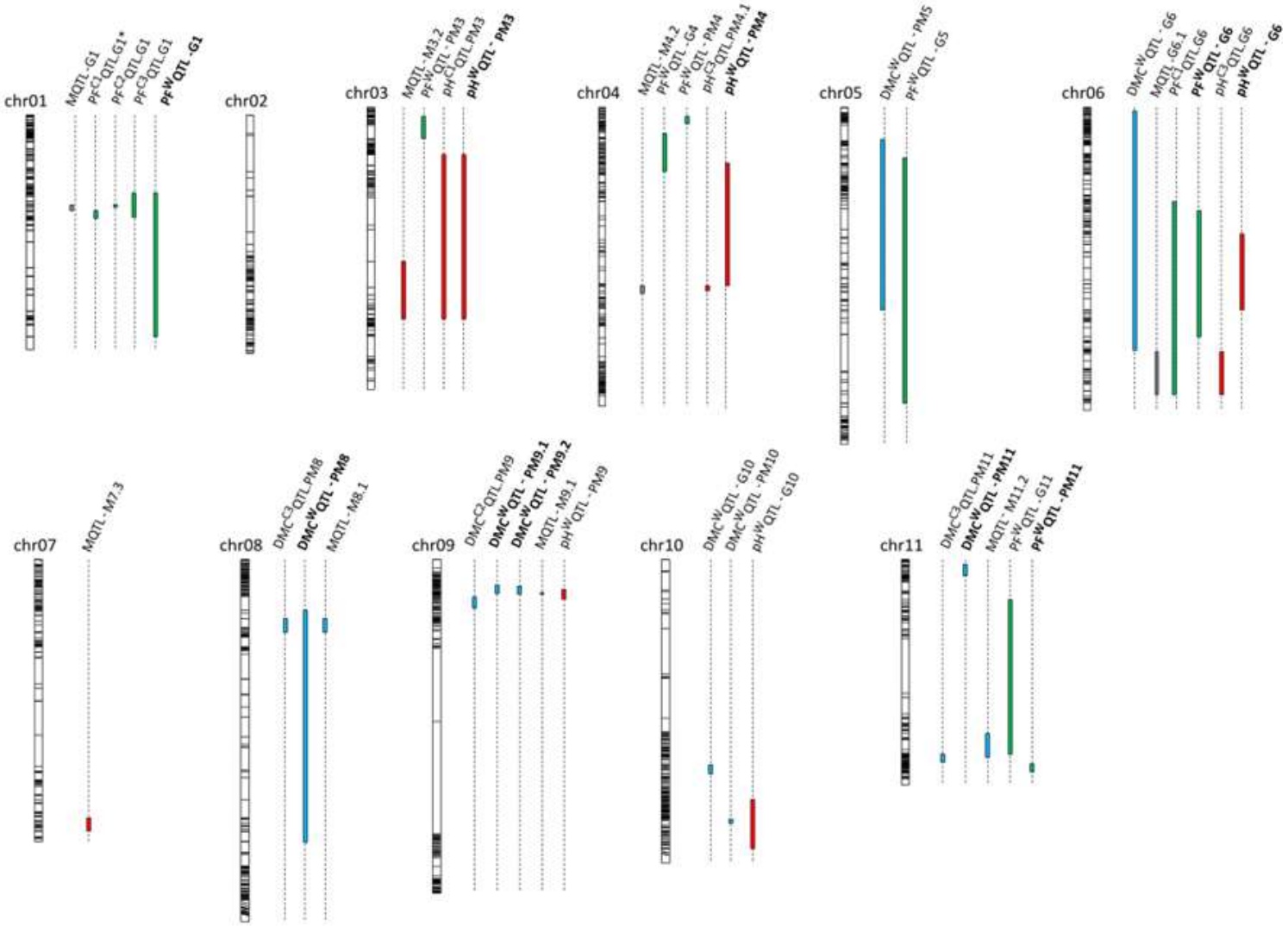
chr01
MQTL-G1
PFCLQTL.G1*
PFCQTL.G1
PFCQTL.G1
PFWQTL-G1
chr02
chr03
MQTL-M3.2
PFWQTL-PM3
pHCQTL.PM3
pHWQTL-PM3
chr04
MQTL-M4.2
PFWQTL-G4
PFWQTL-PM4
pHCQTL.PM4.1
pHWQTL-PM4
chr05
DMCWQTL-PM5
PFWQTL-G5
chr06
DMCWQTL-G6
MQTL-G6.1
PFCQTL.G6
PFWQTL-G6
pHCQTL.G6
pHWQTL-G6
chr07
MQTL-M7.3
chr08
DMCCQTL.PM8
DMCWQTL-PM8
MQTL-M8.1
chr09
DMCCQTL.PM9
DMCWQTL-PM9.1
DMCWQTL-PM9.2
MQTL-M9.1
pHWQTL-PM9
chr10
DMCWQTL-G10
DMCWQTL-PM10
pHWQTL-G10
chr11
DMCCQTL.PM11
DMCWQTL-PM11
MQTL-M11.2
PFWQTL-G11
PFWQTL-PM11

Table 1: Variance decomposition for pH, pulp firmness (PF) and pulp dry matter content (DMC) in the studied progeny, and estimated generalized heritability (Cullis and al., 2006). The proportion of variance explained (PVE, in %) by each factor, i.e. progeny individuals, block, production cycle, interactions between two factors, and residuals were calculated as the percentage of the corresponding sum of squares of each variable to the total sum of squares.

	pH	PF	DMC
Individuals	39.0***	12.2***	61.3***
Block	6.3	0.4	1.5
Cycle	3.2	3.9	0.0
Hybrid*Day	14.5***	23.4***	7.5***
Hybrid*Cycle	15.4***	18.5***	13.7***
Residual	21.6***	41.5***	16.0***
Generalized Heritability	0.77	0.46	0.81

*P< 0.005; **P< 0.01; ***P< 0.001

Table 2: Correlation between quality traits, i.e. pulp pH, firmness (PF) and dry matter content (DMC) at the various studied fruit ripening days

	day 0	day 1		day 2	day 3		day 4	day 5	day 6	day 7	
	PF	PF	pH	PF	PF	pH	PF	PF	PF	PF	pH
pH	0.32***	0.48***	na	0.45***	0.48***	na	0.35***	0.3***	0.31***	0.23***	na
DMC	na	0.39***	0.33***	na	0.3***	0.24***	na	na	na	0.36***	0.09

***P < 0.001

Table 3: Description of QTLs detected in both QTL mapping approaches and the meta-analysis, and QTLs from the first approach (whole dataset) with an R^2 higher than 15%. The day of fruit ripening, trait variability explained by the QTL (R^2), position (Pos), identification (ID), including the quality trait, i.e. pulp pH, firmness (PF) and the dry matter content (DMC), dataset, origin of linkage groups with Galeo (G) and Pisang Madu (PM), and candidate genes colocated with the QTLs are indicated.

Trait	QTL Mapping Approach 1				QTL Mapping Approach 2				Meta-analysis			Candidate genes
	QTL ID	Day	R^2	Pos	QTL ID	Day	R^2	Pos	MQTLs	Pos	Quality traits	
					pH^{C1}QTL-PM1_7	0567	[13.39-33.47]	56.85				
	pH^{W}QTL-PM1_7.1	01234567	[19.27-50.64]	54.94	pH^{C2}QTL-PM1_7.2	567	[16 - 27.5]	58.85	MQTL-PM1_7.2	55.05	pH, PF, DMC	
					pH^{C3}QTL-PM1_7.1	7	15.4	54.2				
pH	pH^{W}QTL-PM1_7.2	0123457	[3.17-6.92]	93.85	pH^{C3}QTL-PM1_7.2	0	22.74	80	MQTL-PM1_7.3	90.53	pH	Aco; GAD; Mal; POX; PEPCK; PEPC
	pH^{W}QTL-PM3	0	8.96	64.00	pH^{C1}QTL-PM3	0	13.47	65	MQTL-PM3.2	64.66	pH	Aco; POX; AG; V-ATPase
	pH^{W}QTL-PM4	4567	[2.25-9.13]	68.24	pH^{C3}QTL-PM4.1	5	18.21	78	MQTL-PM4.2	78.01	pH, PF	Aco; PEPC; AuxREs
	pH^{W}QTL-G6	01234567	[5.56-14.41]	111.9	pH^{C3}QTL-G6	3	24.52	152				
					PF^{C1}QTL-G1*	67	[5.48 - 11.79]	82.42				
	PF^{W}QTL-G1	36	[8.92-9.25]	82.68	PF^{C2}QTL-G1	6	[9.28-15.46]	74.38	MQTL-G1	78.06	pH, PF	GAD; POX
PF					PF^{C3}QTL-G1	3	9.97	72.06				
	PF^{W}QTL-G6	155	[8.24-30.00]	113.84	PF^{C1}QTL-G6	7	9.62	136	MQTL-G6.1	149.20		Aco; CW; CW organization; POX; Mal; PEPCK; PEPC
	PF^{W}QTL-PM11	67	[14.19-17.8]	87.09								POX
	DMC^{W}QTL-PM8	1	9.85	65.49	DMC^{C3}QTL-PM8	7	22.37	63.23	MQTL-PM8.1	63.94	DMC	Aco; CW
	DMC^{W}QTL-PM9.1	13	[17.95-22.10]	11.18								
DMC	DMC^{W}QTL-PM9.2	7	26.12	16.00	DMC^{C2}QTL-PM9	3	26.12	16	MQTL-PM9.1	14.92	pH, PF, DMC	CW
	DMC^{W}QTL-PM11	3	13.49	50.00	DMC^{C3}QTL-PM11	1	27.38	73	MQTL-PM11.2	69.19	DMC	CW; AT; ETR; Gibberellin; UDP; CW biogenesis

Abbreviations for candidate genes: Aco, aconitate hydratase activity; AuxREs, response to auxin; CW, cell wall; ETR, response to ethylene; GAD, Glu decarboxylase; Mal, malate metabolic process; PEPC, phosphoenolpyruvate carboxylase activity; PEPCK, phosphoenolpyruvate carboxykinase (ATP) activity; POX, peroxidase activity; V-ATPase, vacuolar proton-transporting V-type ATPase complex